

Surmounting Oscillating Barriers

Jörg Lehmann, Peter Reimann, and Peter Hänggi

Universität Augsburg, Institut für Physik, Universitätsstr. 1, D-86135 Augsburg, Germany

Thermally activated escape over a potential barrier in the presence of periodic driving is considered. By means of novel time-dependent path-integral methods we derive asymptotically exact weak-noise expressions for both the *instantaneous* and the *time-averaged* escape rate. The agreement with accurate numerical results is excellent over a wide range of driving strengths and driving frequencies.

PACS numbers: 05.40.-a, 82.20.Mj, 82.20.Pm

The problem of noise driven escape over a potential barrier is ubiquitous in natural sciences [1]. Typically, the noise is weak and the escape time is governed by an exponentially leading Arrhenius factor. This scheme, however, meets formidable difficulties in far from equilibrium systems due to the extremely complicated interplay between *global* properties of the metastable potential and the noise [1,2]. Prominent examples are systems driven by time-periodic forces [3,4], exemplified by strong laser driven semiconductor heterostructures, stochastic resonance [5], directed transport in rocked Brownian motors [6], or periodically driven “resonant activation” processes [7] like AC driven biochemical reactions in protein membranes. Despite its experimental importance, the theory of oscillating barrier crossing is still in its infancy. Previous attempts have been restricted to weak (linear response), slow (adiabatic regime), or fast (sudden regime) driving [3–5]. In this Letter we address the most challenging regime of *strong and moderately fast* driving by means of path-integral methods. In fact, our approach becomes asymptotically exact for any finite amplitude and period of the driving as the noise strength tends to zero, and comprises a conceptionally new, systematic treatment of the *rate prefactor* multiplying the exponentially leading Arrhenius factor. Closest in spirit is the recent work [4], which is restricted, however, to the linear response regime for the exponentially leading part and treats the prefactor with a matching procedure, involving the barrier region only. Our analytical theory is tested for a sinusoidally rocked metastable potential against very precise numerical results. Conceptionally, our approach should be of considerable interest for many related problems: generalizations for higher dimensional systems and for non-periodic driving forces.

Model — We consider the overdamped escape dynamics of a Brownian particle $x(t)$ in properly scaled units

$$\dot{x}(t) = F(x(t), t) + \sqrt{2D} \xi(t) , \quad (1)$$

with unbiased δ -correlated Gaussian noise $\xi(t)$ (thermal fluctuations) of strength D . The force-field $F(x, t)$ is assumed to derive from a metastable potential with a well at \bar{x}_s and a barrier at $\bar{x}_u > \bar{x}_s$, subject to periodic mod-

ulations with period \mathcal{T} . For $D = 0$, the deterministic dynamics (1) is furthermore assumed to exhibit a stable periodic orbit (attractor) $x_s(t)$ and an unstable periodic orbit (basin boundary) $x_u(t) > x_s(t)$.

For weak noise D , there is a small probability that a particle obeying (1) escapes from the basin of attraction $\mathcal{A}(t) := (-\infty, x_u(t)]$ of $x_s(t)$ and disappears towards infinity. For an ensemble of particles with probability density $p(x, t)$, the population $P_{\mathcal{A}}(t)$ within the basin of attraction is $\int_{-\infty}^{x_u(t)} p(x, t) dx$ and the instantaneous rate of escape $\Gamma(t)$ equals $-\dot{P}_{\mathcal{A}}(t)/P_{\mathcal{A}}(t)$. Apart from transients at early times, this rate $\Gamma(t)$ is independent of the initial conditions at time t_0 . Without loss of generality we can thus focus on $x(t_0) = x_s(t_0)$. Small D implies rare escape events, i.e. the deviation of $P_{\mathcal{A}}(t)$ from its initial value $P_{\mathcal{A}}(t_0) = 1$ is negligible. Exploiting $\dot{x}_u(t) = F(x_u(t), t)$ and the Fokker-Planck-equation $\partial_t p = \partial_x \{-F(x, t) + D\partial_x\} p$ governing $p = p(x, t)$ we find for the instantaneous rate

$$\Gamma(t) = -D \partial_x p(x = x_u(t), t) . \quad (2)$$

Path-integral approach — With the choice $p(x, t_0) = \delta(x - x_s(t_0))$ we obtain for the conditional probability $p(x, t)$ the path integral representation [8]

$$p(x_f, t_f) = \int \mathcal{D}x(t) e^{-S[x(t)]/D} , \quad (3)$$

where the “action” is given by

$$S[x(t)] := \int_{t_0}^{t_f} dt [\dot{x}(t) - F(x(t), t)]^2/4 \quad (4)$$

and where $x(t_0) = x_s(t_0)$ and $x(t_f) = x_f$ are the “initial” and “final” conditions for the paths $x(t)$. For weak noise, the integral (3) is dominated by a set of paths $x_k^*(t)$, corresponding to minima of the action (4) (distinguished by the label k). These satisfy an Euler-Lagrange equation equivalent to the following Hamiltonian dynamics

$$\dot{p}_k^*(t) = -p_k^*(t) F'(x_k^*(t), t) \quad (5)$$

$$\dot{x}_k^*(t) = 2p_k^*(t) + F(x_k^*(t), t) \quad (6)$$

with $F'(x, t) := \partial_x F(x, t)$. For well separated paths $x_k^*(t)$, a functional saddle point approximation in (3) yields

$$p(x_f, t_f) = \sum_k \frac{e^{-S[x_k^*(t)]/D}}{[4\pi D Q_k^*(t_f)]^{1/2}} [1 + \mathcal{O}(D)] , \quad (7)$$

where the quantity $Q_k^*(t)$ relates to the determinant of fluctuations around $x_k^*(t)$. Following the reasoning in [9], we find for our case [10] that $Q_k^*(t)$ obeys the relation

$$\begin{aligned} \ddot{Q}_k^*(t)/2 - d[Q_k^*(t)F'(x_k^*(t), t)]/dt \\ + Q_k^*(t)p_k^*(t)F''(x_k^*(t), t) = 0 \end{aligned} \quad (8)$$

with initial conditions $Q_k^*(t_0) = 0$ and $\dot{Q}_k^*(t_0) = 1$. Exploiting that the derivative of the action at its end-point equals the momentum $p_k^*(t_f)$, we can infer from (2,7) our first main result, namely

$$\Gamma(t_f) = \sum_k \frac{p_k^*(t_f) e^{-S[x_k^*(t)]/D}}{[4\pi D Q_k^*(t_f)]^{1/2}} [1 + \mathcal{O}(D)] , \quad (9)$$

where the boundary conditions $x_k^*(t_0) = x_s(t_0)$ and $x_k^*(t_f) = x_u(t_f)$ are understood in (5,6). In view of (7), the instantaneous rate (9) has the suggestive form of probability at the separatrix times “velocity”.

Closer inspection of (4-6) reveals the following generic features of each path $x_k^*(t)$ which notably contributes to the rate (9), see fig. 1: Starting at $x_k^*(t_0) = x_s(t_0)$, it continues to follow rather closely the stable periodic orbit $x_s(t)$ for some time. At a certain moment, it crosses over into the vicinity of the unstable periodic orbit $x_u(t)$ and remains there for the rest of its time, ending at $x_k^*(t_f) = x_u(t_f)$. Without loss of generality, we can sort the paths $x_k^*(t)$ by the time they spend near the unstable periodic orbit, such that $x_0^*(t)$ is that path which crosses over from $x_s(t)$ to $x_u(t)$ at the “latest possible moment”. Apart from a time shift, each path $x_k^*(t)$ then closely resembles the same “master path” $x^*(t)$ (see fig. 1). This path $x^*(t)$ is defined as an absolute minimum of the action (4) in the limit $t_0 \rightarrow -\infty$, $t_f \rightarrow \infty$, and is fixed uniquely by demanding that $x^*(t + k\mathcal{T})$ is the “master path” associated with $x_k^*(t)$.

The basic qualitative features of each minimizing path $x_k^*(t)$ are thus quite similar to the well-known barrier-crossing problem in a static potential [11]. However, in the limit $t_0 \rightarrow -\infty$, $t_f \rightarrow \infty$ we have, in contrast to this latter situation, *not* a continuous symmetry (Goldstone mode), but a *discrete degeneracy* of the minimizing paths. As a consequence, in our case the minimizing paths $x_k^*(t)$ remain well separated and thus the rate formula (9) is valid for any (arbitrary but fixed) finite values of the driving amplitude and period, provided the noise strength D is sufficiently small. On the other hand, for a given D we have to exclude extremely small amplitudes and extremely long or short periods since this would lead effectively back to the static case.

As long as the “master path” $x^*(t)$ remains sufficiently close to the stable periodic orbit $x_s(t)$, say for $t \leq t_s$, the force-field is well approximated by

$$F(x, t) = F(x_s(t), t) + (x - x_s(t))F'(x_s(t), t) . \quad (10)$$

An analogous approximation for $F(x, t)$ is valid while $x^*(t)$ remains in a sufficiently small neighborhood of $x_u(t)$, say for $t \geq t_u$. The corresponding local solutions of the Hamilton equations (5,6) can then be written as

$$p^*(t) = p^*(t_{s,u}) e^{-\Lambda_{s,u}(t, t_{s,u})} \quad (11)$$

$$x^*(t) = x_{s,u}(t) \pm p^*(t) I_{s,u}(t) . \quad (12)$$

Here ‘ s, u ’ means that the index is either ‘ s ’ or ‘ u ’ and the upper and lower signs in (12) refer to ‘ s ’ and ‘ u ’, respectively. Further, we have introduced

$$\Lambda_{s,u}(t, t_{s,u}) := \int_{t_{s,u}}^t F'(x_{s,u}(\hat{t}), \hat{t}) d\hat{t} \quad (13)$$

$$I_{s,u}(t) := \left| 2 \int_{\mp\infty}^t e^{2\Lambda_{s,u}(t, \hat{t})} d\hat{t} \right| . \quad (14)$$

Similarly, the local solutions for the prefactor in (8) can be written as

$$Q^*(t \leq t_s) = I_s(t)/2 \quad (15)$$

$$Q^*(t \geq t_u) = c_1/p^*(t)^2 - c_2 I_u(t) . \quad (16)$$

The parameters $p^*(t_{s,u})$ in (11) and $c_{1,2}$ in (16) cannot be fixed within such a local analysis around $x_{s,u}(t)$, they require the global solution of (5,6,8). We furthermore observe that due to the time-periodicity of $F(x, t)$ and $x_{s,u}(t)$, the quantities

$$\lambda_{s,u} := \Lambda_{s,u}(t + \mathcal{T}, t)/\mathcal{T} \quad (17)$$

are indeed t -independent. The stability/instability of the periodic orbits $x_{s,u}(t)$ implies $\lambda_s < 0$ and $\lambda_u > 0$. It follows that $I_{s,u}(t)$ from (14) are finite, \mathcal{T} -periodic functions.

The expressions for $x_k^*(t)$, $p_k^*(t)$, and $Q_k^*(t)$ are somewhat more complicated than in (11-16) but since $x_k^*(t)$ is well approximated by $x^*(t + k\mathcal{T})$, the same follows for $p_k^*(t)$ and $Q_k^*(t)$. Closer inspection shows [10] that in (9) the pre-exponential factors $p_k^*(t_f)$ and $Q_k^*(t_f)$ can be approximated by $p^*(t_f + k\mathcal{T})$ and $Q^*(t_f + k\mathcal{T})$ without further increasing the error $\mathcal{O}(D)$ in (9). Within this same accuracy, the exponential in (9) requires – due to the small denominator D – a somewhat more elaborate approximation, yielding

$$S[x_k^*(t)] = S[x^*(t)] + \int_{t_f + k\mathcal{T}}^{\infty} p^*(t)^2 dt . \quad (18)$$

Rate formula — By introducing these approximations into (9), exploiting (11-16), and dropping the index ‘ f ’ of t_f , we obtain [10] as the central result of this work the *instantaneous rate*

$$\Gamma(t) = \sqrt{D} \alpha e^{-S[x^*(t)]/D} \kappa(t, D) [1 + E(D)] \quad (19)$$

$$\alpha := [4\pi \mathcal{T}^2 \lim_{t \rightarrow \infty} p^*(t)^2 Q^*(t)]^{-1/2} \quad (20)$$

$$\kappa(t, D) := \mathcal{T} \sum_{k=-\infty}^{\infty} \frac{\beta_k(t)^2}{D} e^{-\beta_k(t)^2 I_u(t)/2D} \quad (21)$$

$$\beta_k(t) := e^{-\lambda_u k\mathcal{T}} \lim_{\hat{t} \rightarrow \infty} p^*(\hat{t}) e^{\Lambda_u(\hat{t}, t)} . \quad (22)$$

The relative error $E(D)$ is found to be of order $\mathcal{O}(D)$ if $F''(x_u(t), t) \equiv 0$, and $\mathcal{O}(D^{1/2})$ otherwise. By use of (13-17) one finds that the average of (21) over a single

time-period \mathcal{T} equals 1. For the *time-averaged rate* $\bar{\Gamma}$ we thus obtain

$$\bar{\Gamma} = \sqrt{D} \alpha e^{-S[x^*(t)]/D} [1 + E(D)]. \quad (23)$$

It consists of an Arrhenius-type exponentially leading part and, *in contrast to equilibrium rates* [1], a non-trivial pre-exponential D -dependence.

An archetype example — In general, the explicit quantitative evaluation of $S[x^*(t)]$, α , and $\kappa(t, D)$ in (19,23) is not possible in closed analytical form. An exception is the piecewise linear force-field with additive sinusoidal driving

$$\begin{aligned} F(x \leq 0, t) &= \lambda_s (x - \bar{x}_s) + A \sin(\Omega t) \\ F(x \geq 0, t) &= \lambda_u (x - \bar{x}_u) + A \sin(\Omega t), \end{aligned} \quad (24)$$

corresponding to a periodically rocked piecewise parabolic potential, with parameters $\bar{x}_s < 0$, $\bar{x}_u > 0$, $\lambda_s < 0$, $\lambda_u > 0$, respecting $\lambda_s \bar{x}_s = \lambda_u \bar{x}_u$ (continuity at $x = 0$). To simplify the analytical calculations we further restrict ourselves to the case that the “master path” $x^*(t)$ crosses the matching point $x = 0$ in (24) only once [12], say at $t = t_c$. The periodic orbits $x_{s,u}(t)$ then assume the simple form

$$x_{s,u}(t) = \bar{x}_{s,u} - \frac{A [\lambda_{s,u} \sin(\Omega t) + \Omega \cos(\Omega t)]}{\lambda_{s,u}^2 + \Omega^2}. \quad (25)$$

Moreover, Eqs.(11,12) are now valid with index ‘ s ’ for all $t \leq t_c$ and with ‘ u ’ for all $t \geq t_c$. By matching these solutions at $t = t_c$ the global parameters $p^*(t_{s,u})$ in (11) are fixed and one obtains

$$t_c = \frac{1}{\Omega} \arctan \left(\frac{\lambda_u \lambda_s - \Omega^2}{\Omega (\lambda_u + \lambda_s)} \right). \quad (26)$$

To ensure that $x^*(t)$ is a minimum of the action in (4) one has

$$(\lambda_u + \lambda_s) A \Omega \cos(\Omega t_c) < 0. \quad (27)$$

In the same manner, the prefactor (16) has to be matched at $t = t_c$. While $Q^*(t)$ is still continuous, $\dot{Q}^*(t)$ develops a jump at $t = t_c$ which can be determined from (8). Upon collecting everything, the final result reads

$$S[x^*(t)] = \Delta V \left[1 - \frac{|A \lambda_u \lambda_s|}{(R \Delta V)^{1/2}} \right]^2 \quad (28)$$

$$\alpha = \left[\frac{|A|(\Omega^2 + \lambda_u \lambda_s) + (R \Delta V)^{1/2}}{16 \pi^3 |A| S[x^*(t)]} \right]^{1/2} \quad (29)$$

$$\beta_k(t) = e^{-\lambda_u (k\mathcal{T} + t - t_c)} \left[\lambda_u \bar{x}_u - \frac{|A \lambda_u \lambda_s|}{H^{1/2}} \right], \quad (30)$$

where $H := (\lambda_u^2 + \Omega^2)(\lambda_s^2 + \Omega^2)$, $R := 2H/(\lambda_u^{-1} - \lambda_s^{-1})$, and $\Delta V := (\lambda_u \bar{x}_u^2 - \lambda_s \bar{x}_s^2)/2$ is the potential barrier corresponding to the undriven ($A = 0$) force-field (24). With

$\mathcal{T} = 2\pi/\Omega$, $I_u(t) = 1/\lambda_u$, and t_c from (26,27), the rate (19,23) is thus determined completely.

Comparison — These analytical predictions for the instantaneous rate (19) are compared in fig. 2 for a representative set of parameter values with very accurate numerical results. The agreement indeed improves with decreasing noise-strength D . While the absolute values of $\Gamma(t)$ and the location of the extrema strongly depend on D , the overall shape changes very little and does *not* develop singularities as $D \rightarrow 0$. The corresponding time-averaged rates (23) are depicted in fig.3, exhibiting excellent agreement between theory and numerics even for relatively large D . The inset of fig. 3 confirms our prediction that the relative error $E(D)$ in (23) decreases asymptotically like D . Finally, fig.4. illustrates the dependence of the averaged rate $\bar{\Gamma}$ upon the amplitude A of the periodic driving force. As expected, our theoretical prediction compares very well with the (numerically) exact rate, except for very small driving amplitudes A (see the discussion above eq. (10)). The approximation from [4] is complementary to ours in that it is very accurate for small A but develops considerable deviations with increasing A . Those approximations have been omitted in figs.2,3 since they are not valid in this parameter regime and indeed are way off.

This work was supported by DFG-Sachbeihilfe HA1517/13-2 and the Graduiertenkolleg GRK283.

-
- [1] P. Hänggi, P. Talkner, and M. Borkovec, Rev. Mod. Phys. **62**, 251 (1990).
 - [2] R. Graham and T. Tél, Phys. Rev. A **31**, 1109 (1985); S.J.B. Einchcomb and A.J. McKane, Phys. Rev. E **51**, 2974 (1995); R.S. Maier and D.L. Stein, SIAM J. Appl. Math. **57**, 752 (1997).
 - [3] R. Graham and T. Tél, J. Stat. Phys. **35**, 729 (1984); P. Jung, Phys. Rep. **234**, 175 (1993); P. Talkner, New J. Phys. **1**, 4 (1999).
 - [4] V.N. Smelyanskiy, M.I. Dykman, and B. Golding, Phys. Rev. Lett. **82**, 3193 (1999).
 - [5] L. Gammaitoni, P. Hänggi, P. Jung, and F. Marchesoni, Rev. Mod. Phys. **70**, 223 (1998).
 - [6] R.D. Astumian, Science **276**, 917 (1997); F. Jülicher, A. Ajdari, and J. Prost, Rev. Mod. Phys. **69**, 1269 (1997).
 - [7] C.R. Doering and J.C. Gadoua, Phys. Rev. Lett. **69**, 2318 (1992); for a review see: P. Reimann and P. Hänggi in *Stochastic Dynamics*, Lecture Notes in Physics, Vol. **484**, L. Schimansky-Geier and Th. Pöschel (eds.), Springer, Berlin 1997; pp 127-139.
 - [8] M.I. Freidlin and A.D. Wentzell, *Random Perturbations of Dynamical Systems*, Springer, New York 1984.
 - [9] L.S. Schulman, *Techniques and Applications of Path Integration* Wiley, New York 1981.
 - [10] Details will be presented elsewhere.
 - [11] B. Caroli, C. Caroli, and B. Roulet, J. Stat. Phys. **26**, 83

(1981); U. Weiss, Phys. Rev. A **25**, 2444 (1982).

[12] In general, the self-consistency of the final solution $x^*(t)$ with this assumption has to be checked numerically (a transcendental equation arises). Analytically, one can show that $A^2 < \lambda_{s,u}^2 \bar{x}_{s,u}^2$ is a sufficient (but not necessary) condition, while $A^2 < (\lambda_{s,u}^2 + \Omega^2) \bar{x}_{s,u}^2$ is necessary but not sufficient. The latter inequality also guarantees that the expressions in the square brackets in (28-30) are positive.

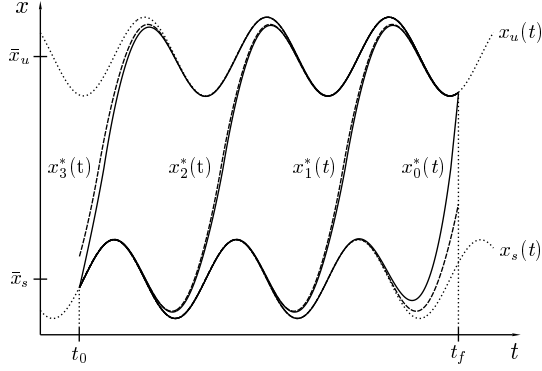


FIG. 1. Solid: The paths $x_k^*(t)$, $k = 0, \dots, 3$, which minimize the action (4) with boundary conditions $x_k^*(t_0) = x_s(t_0)$ and $x_k^*(t_f) = x_u(t_f)$ for the example (24) with $\bar{x}_s = \lambda_s = -1$, $\bar{x}_u = \lambda_u = \Omega = 1$, $A = 0.5$ (dimensionless units). Dashed: the associated “master paths” $x^*(t + k\mathcal{T})$. Dotted: stable and unstable periodic orbits $x_s(t)$ and $x_u(t)$. In this plot, $t_f - t_0$ has been chosen rather small. As $t_f - t_0$ increases, more and more intermediate paths $x_k^*(t)$ appear which better and better agree with $x^*(t + k\mathcal{T})$.

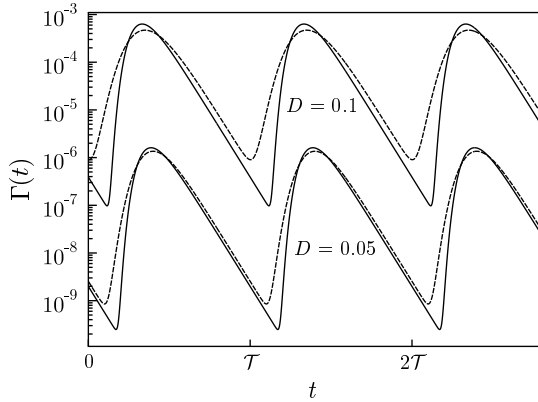


FIG. 2. Instantaneous rate $\Gamma(t)$ for the force field (24) with $\bar{x}_s = \lambda_s = -1$, $\bar{x}_u = \lambda_u = \Omega = 1$, $A = 0.5$, corresponding to a static ($A = 0$) potential barrier $\Delta V = 1$. Solid: analytical result (19,21,26-30). Dashed: high-precision numerical results by evolving the Fokker-Planck-equation for $p(x, t)$ until transients have died out and then evaluating (2).

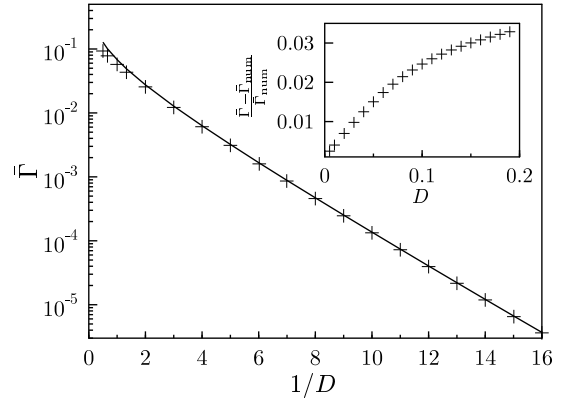


FIG. 3. Arrhenius plot of the time-averaged rate $\bar{\Gamma}$. Parameters are like in fig.2. Solid: analytical result (23,28,29). Crosses: precise numerical results. Inset: relative difference between analytical ($\bar{\Gamma}$) and numerical ($\bar{\Gamma}_{\text{num}}$) rate.

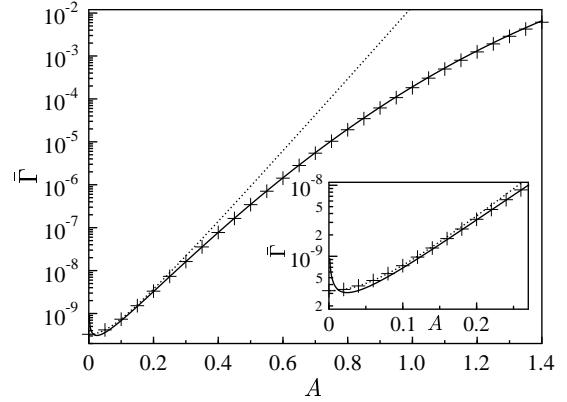


FIG. 4. Time-averaged rate $\bar{\Gamma}$ vs. driving amplitude A for $D = 0.05$. Parameters are like in fig.2. Crosses: precise numerical results. Solid: analytical result (23,28,29). Dotted: theoretical approximation from Ref. [4]. The small- A regime is magnified in the inset.